THE ASTROPHYSICAL JOURNAL, 246:L155–L159, 1981 June 15

ORIGIN AND LOCATION OF THE HARD X-RAY EMISSION IN A TWO-RIBBON FLARE

P. HOYNG,[1] A. DUIJVEMAN,[1] M. E. MACHADO,[2] D. M. RUST,[3] Z. SVESTKA,[1] A. BOELEE,[1]
C. DE JAGER,[1] K. J. FROST,[4] H. LAFLEUR,[1] G. M. SIMNETT,[5]
H. F. VAN BEEK,[1] AND B. E. WOODGATE[4]
Received 1980 December 22; accepted 1981 February 27

ABSTRACT

We report observations on the two-ribbon flare of 1980 May 21 by the Hard X-Ray Imaging Spectrometer, the Hard X-Ray Burst Spectrometer, and the UV Spectrometer and Polarimeter aboard the *Solar Maximum Mission*, as well as Hα and magnetic field data. Our conclusions are (1) the impulsive 16–30 keV X-ray spike bursts originated from separate locations of $\sim 8''$ width, coinciding in position with Hα flare kernels. This hard X-ray emission was caused by beams of accelerated electrons. (2) The impulsive spike bursts came from the footpoints of loops arched over a $30''$ region where new magnetic flux emerged, which caused eruption of a filament immediately before the flare. (3) Temperatures in excess of 7×10^7 K were observed during the thermal phase. The hot plasma component cooled by anomalous heat conduction, requiring a continuous energy release of $\sim 2 \times 10^{29}$ ergs s^{-1} initially, to $\sim 4 \times 10^{28}$ ergs s^{-1} later on.

Subject headings: Sun: flares — Sun: X-rays

I. INTRODUCTION

On 1980 May 21 a 2B/X1 two-ribbon flare occurred in AR 2456 at S13 W15, beginning around $20^{h}50^{m}$ UT. This flare was well observed by a number of *SMM* experiments. High-resolution magnetograms and Hα images are also available. In this *Letter* we describe and analyze the data from the Hard X-Ray Imaging Spectrometer (HXIS), also using observations from the Hard X-Ray Burst Spectrometer (HXRBS), and the UV Spectrometer Polarimeter (UVSP) aboard the *SMM*, as well as Kitt Peak magnetograms and Holloman and Boulder Hα filtergrams. For details on the HXIS instrument we refer to van Beek *et al.* (1980, 1981); for HXRBS see Orwig, Frost, and Dennis (1980), and for UVSP, Woodgate *et al.* (1981).

II. OBSERVATIONS

a) *Chromospheric and Magnetic Development*

In Hα the flare developed around the breakup points of the dark filament seen in Figure 1*a* (Plate L10) at $19^{h}06^{m}$. The filament broadened and became diffuse near point *A* at $20^{h}45^{m}$. The filament parted at *A* at the time the 8–20 Å X-ray emission began, $20^{h}48^{m}$. By $20^{h}50^{m}38^{s}$ the filament had broken into two distinct sections, which started to rise at $20^{h}52^{m}$, 4 minutes before the hard X-ray burst. Four Hα patches (Fig. 2 [Plate L11]) reached flare kernel brightness at $20^{h}54^{m}50^{s}$. By this time, the central one-third of the filament had disappeared. At $20^{h}56^{m}$ (hard X-ray maximum), the easternmost one-third of the filament was disappearing from the on-band images. Subsequent off-band frames showed material ejected upward and southward out of the flaring region. A type II radio burst was seen by Culgoora and Clark Lake starting at $20^{h}57^{m}$. Bright postflare loops (Fig. 1*c*) appeared over the filament channel shortly after Hα flare maximum, at $21^{h}00^{m}$.

On- and off-band Hα images taken with $1''$ resolution at the Holloman Solar Observatory before and after the flare show clearly that a new sunspot appeared within $5''$ of point *A*, where the filament began to break up. There are no spots within $10''$ of point *A* at $19^{h}06^{m}$, but pictures after $22^{h}00^{m}$ clearly show a $5''$ diameter sunspot in the filament channel at point *A*. We take this to be evidence for the emergence of new magnetic fields beneath the filament. This is confirmed by a sequence of magnetograms obtained with $1''$ resolution at the Kitt Peak National Observatory, Figures 1*b* and 1*d*. An $8''$ knot of negative field (black) appeared in the positive fields bordered by the filament. Comparison of the sunspot pictures with the magnetograms reveals that the new sunspot corresponds to a new positive feature in the magnetogram. The adjacent features, *A* and *B*, show that a bipolar flux region emerged below the filament. Around $20^{h}53^{m}$, HXIS observed a 3.5–8 keV emission

[1] The Astronomical Institute at Utrecht, The Netherlands.
[2] Observatorio de Fisica Cosmica–CNIE, San Miguel, Argentina.
[3] American Science & Engineering, Inc., Cambridge, Massachusetts.
[4] Laboratory for Astronomy and Solar Physics, NASA Goddard Space Flight Center, Maryland.
[5] Department of Space Research, University of Birmingham, England.

1981ApJ...246L.155H

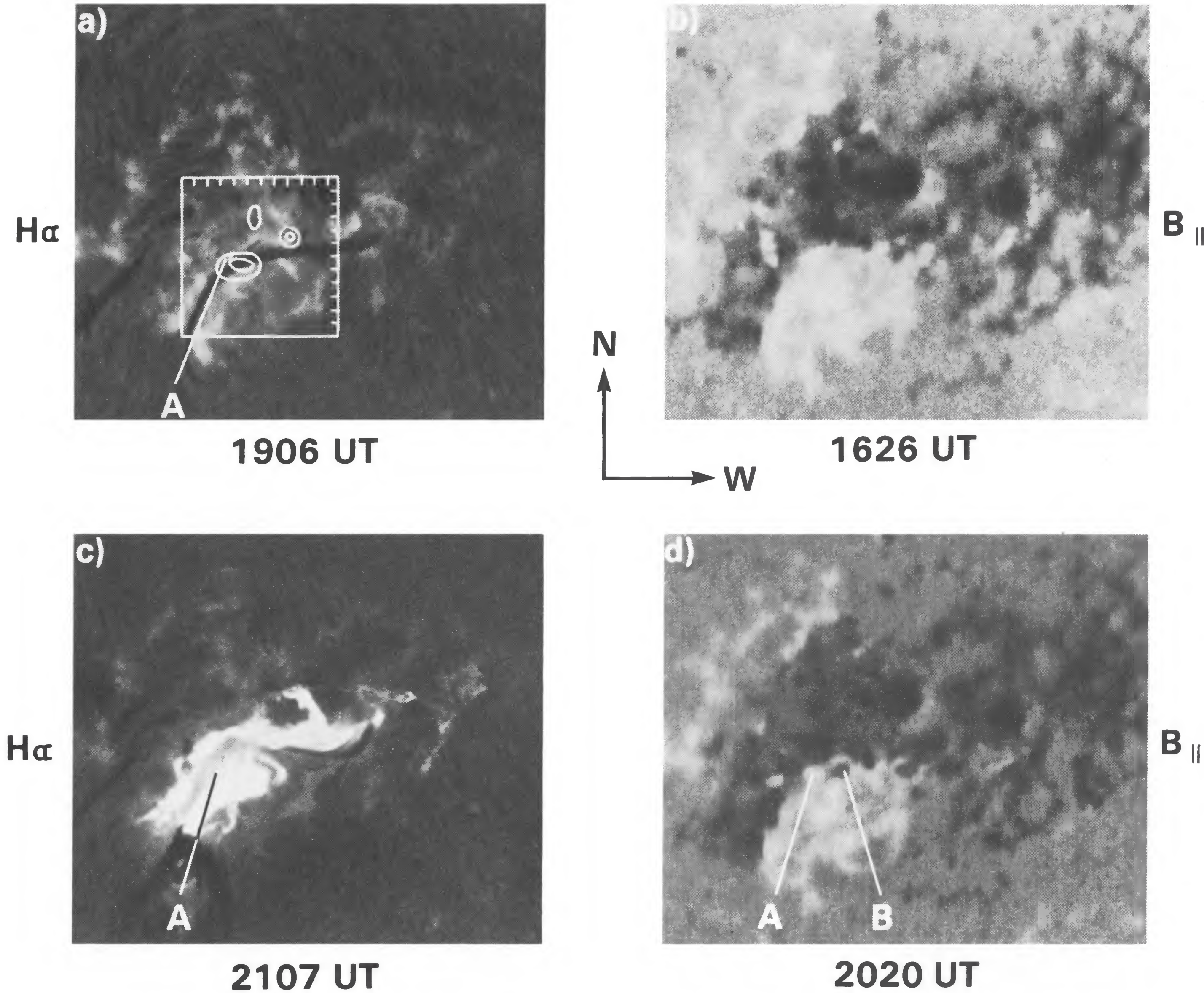

FIG. 1.—The flare of 1980 May 21. (*a*) Hα image at 19^h06^m. The superposed frame measures 96″×96″ and corresponds to the frames used in Fig. 4. (*b*) Line-of-sight component of the underlying magnetic fields at 16^h26^m. (*c*) Hα flare at 21^h07^m. (*d*) Magnetic fields at 20^h20^m. *A* is the location of the new sunspot (positive flux); *B* is the location of new negative flux.

HOYNG *et al.* (*see* page L155)

FLARE KERNELS

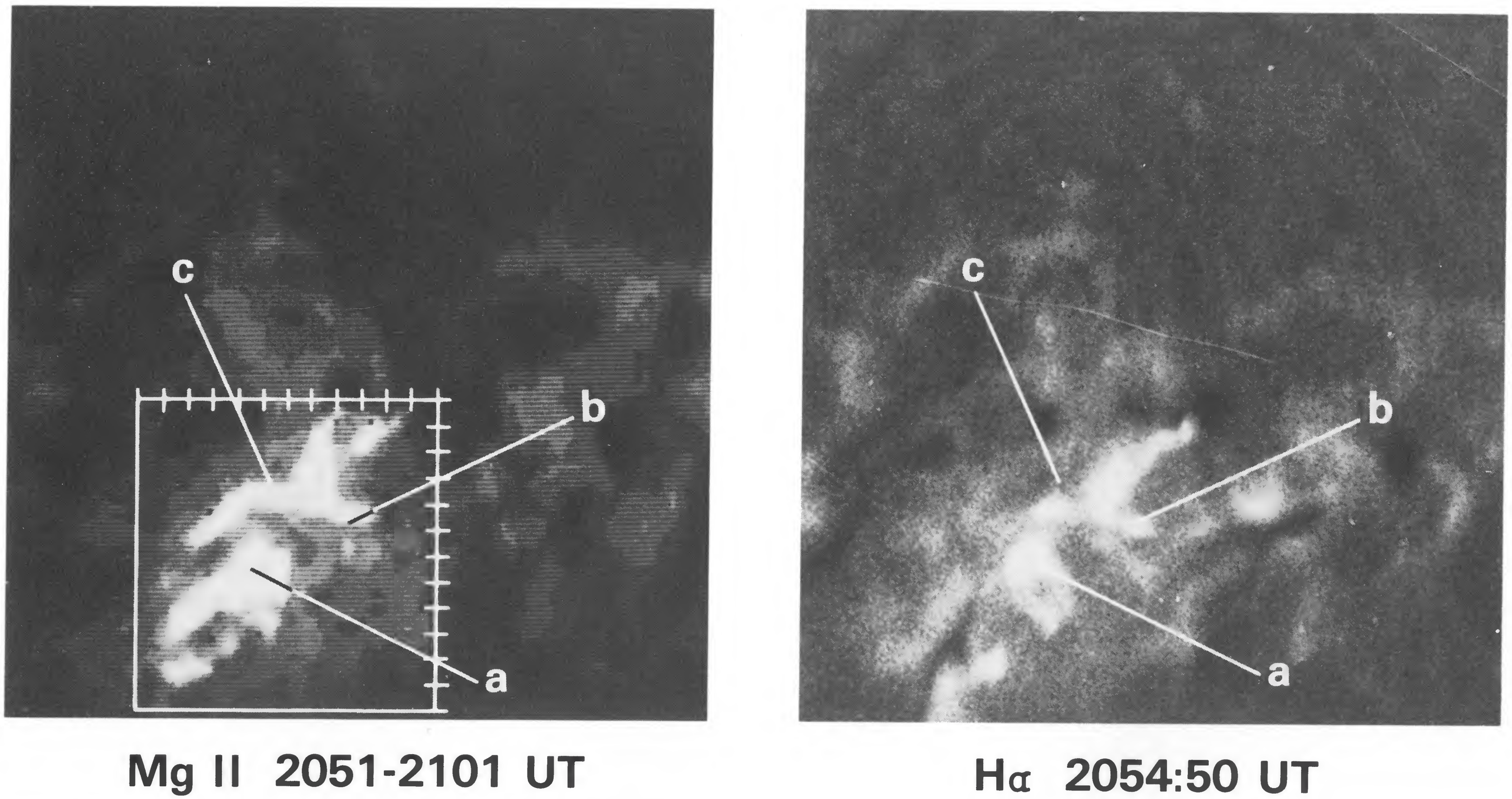

FIG. 2.—The flare kernels of 1980 May 21. *Left:* UVSP Mg II spectroheliogram (λ2795) measuring about 4′ × 4′, obtained by a vertical raster scan starting 20^h51^m in the lower right corner, ending in the upper left at 21^h01^m. The flare area increased as the raster was made, and so the Mg II image does not correspond exactly to the instantaneous Hα image. Pointers mark the centers of the three brightest 8″ × 8″ HXIS pixels involved in the 16 × 30 keV emission around $20^h55^m55^s$ and $20^h56^m25^s$. The superposed frame measures 96″ × 96″, and it shows the position of the frames used in Fig. 2. The overlay of the HXIS and UVSP fields of view is based on offsets between both instruments measured during flight. *Right:* Boulder flare patrol Hα frame at $20^h54^m50^s$. Points *a*, *b*, and *c* indicate the centers of the three most important HXIS pixels involved in the 16–30 keV emission around 20^h56^m. Allowing for the usual drift of flare kernels away from the center of the flare, the HXIS emission patches coincide with three Hα kernels.

HOYNG *et al.* (see page L155)

PLATE L11

that clearly outlined the filament and a brightening to ~ 16 keV approximately at the location of new emerging flux.

b) *Hard X-ray Flare*

The hard X-ray time profiles observed with the HXRBS, Figure 3, show a few spikes after which there is a featureless tail. The hard X-ray spectrum softened as time progressed. Figure 4 displays contour plots in two X-ray energy bands at the times indicated with arrows in Figure 3. At the time of peaks 1 and 2, the hard X-rays (16–30 keV) came from two spatially well separated locations, while the softer X-rays (3.5–8 keV) emerged from a broader region in between. The 16–30 keV emission at these two times had also a diffuse component which coincided with the 3.5–8 keV emission patch. At present the true spatial extent of this diffuse 16–30 keV emission is not well known because of an enhanced background. For this reason only two high contours, those definitely unaffected by background, are shown in both 16–30 keV images. The light curves of the two 16–30 keV emission patches around $20^h55^m55^s$ coincide in time to within 3 s. This accuracy is limited by count statistics. The same conclusion holds for both 16–30 keV patches around $20^h56^m25^s$.

The X-ray images at $20^h57^m30^s$ and all later times show that the 16–30 keV source coincided spatially with the 3.5–8 keV source. The centroid of the 16–30 keV emission was displaced $\sim 3''$ to the south with respect to the centroid of the 3.5–8 keV emission. We have also looked for the location of the hard X-ray source in our highest band, 22–30 keV, and find that it coincided with the 16–30 keV source at $20^h57^m30^s$ and later. Both the 3.5–8 keV X-ray source and the 16–30 keV source moved southward together with an apparent velocity of ~ 5 km s^{-1} around 21^h10^m, decreasing slowly as time progressed.

c) *Spatial Relation between Optical and X-ray Flare*

Figure 2 summarizes the position of the three relevant HXIS pixels in a Mg II spectroheliogram (λ2795) by the UVSP around 20^h56^m. This Mg II line is formed in the chromosphere at a level comparable to Hα. The southern 16–30 keV emission around 20^h56^m involves three HXIS pixels of which the middle one, *a*, is the brightest at $20^h55^m55^s$ as well as at $20^h56^m25^s$. The northern 16–30 keV emission emerges from pixel *b* at $20^h55^m55^s$ and from pixel *c* at $20^h56^m25^s$. Since the UVSP-HXIS coalignment is known with an accuracy of $\sim 8''$ in both directions, and since the Mg II and Hα images are sufficiently similar to allow alignment to within $\sim 5''$, we were able to overlay the HXIS field of view with a Hα frame at $20^h54^m50^s$ (Fig. 2). We conclude that three of the Hα flare kernels were within $\sim 8''$ of a hard X-ray emission patch. The association of Hα flare kernels and impulsive X-ray bursts has long been suspected and is hereby confirmed for the first time.

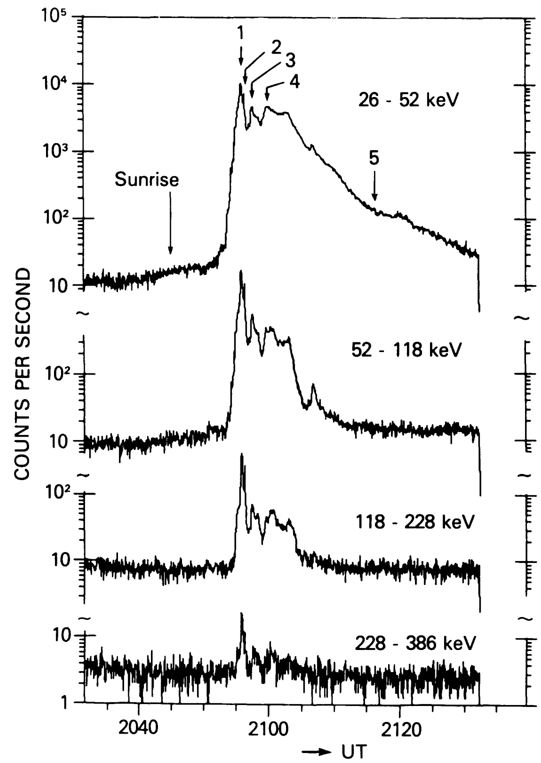

FIG. 3.—Hard X-ray time profiles as observed by HXRBS on 1980 May 21. Sunrise for *SMM* was at 20^h45^m.

III. INTERPRETATION

Our data imply that the emergence of new flux caused the destabilization of the filament and the subsequent flare. We realize that the association could be accidental, but there is strong evidence for a causal relation. The eruption of the filament and gradual brightening of the Hα kernels preceded the hard X-ray and optical flare. In addition, the HXIS flare patches occurred where Hα brightened before the flare. The brightest X-ray flare patch occurred near *A* (Fig. 1), where the new magnetic flux emerged and the filament first broke up. This basic picture of a two-ribbon flare has been proposed by Heyvaerts, Priest, and Rust (1977) (flux emergence and preflare heating) and by Kuperus and Van Tend (1981) (energy release through filament eruption). In the latter theory, emergence of new flux can decrease the strength of the background magnetic field, thus disturbing the balance of forces acting on the filament leading eventually to filament eruption. In the present case, the filament moved also considerably southward as it rose.

1981ApJ...246L.155H

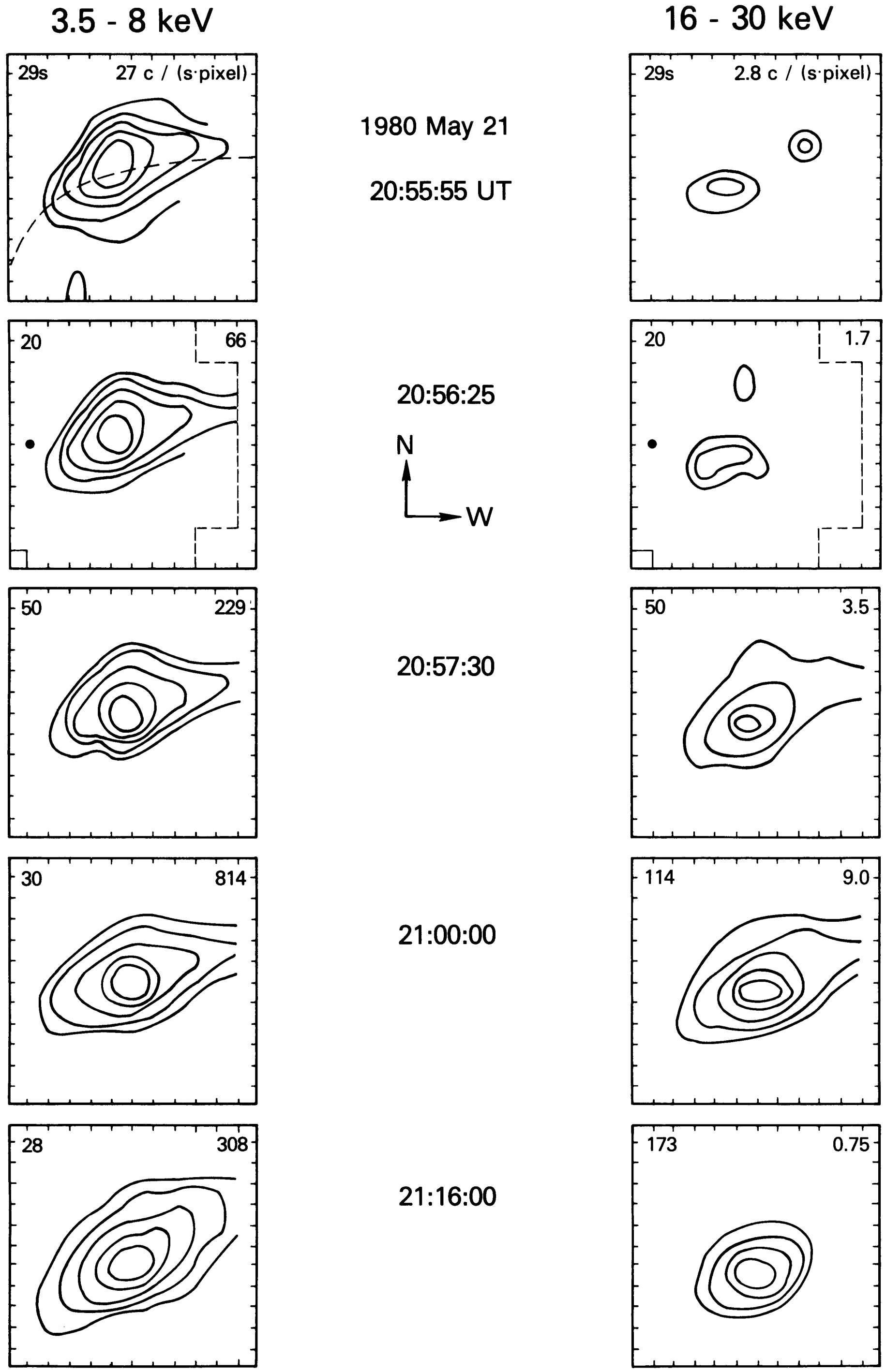

FIG. 4.—X-ray contour plots at the times indicated by arrows in Fig. 3. The contours are at fractions of 3/4, 1/2, 1/4, 1/8, and 1/16 of the maximum brightness. The latter is given at the top right in units of counts s^{-1} per 8″×8″ pixel. Many single HXIS images were added before constructing each contour plot. The integration time in seconds is shown at the top left. The dashed line in the top left figure indicates the position of the filament. Both contour plots at $20^h56^m25^s$ show the center (●) and the boundary (---) of the HXIS fine field of view. The marks on the axes are 8″ apart. In the top right two frames, there is a diffuse emission between the bright points, see text.

The hard X-ray bright points observed around 20^h56^m must have been connected by loops, one connecting the areas near pixels *a* and *b*, and one connecting those near *a* and *c*; see Figure 2 (cf. the Hα loops that were visible shortly after 21^h00^m). These loops either stretched over the rising filament and were activated by it (e.g., internal reconnection—Spicer 1977), or they were formed by violent reconnection under the filament. The thermal phase of the flare set in around 21^h00^m and the subsequent development followed the scenario presented by Moore *et al.* (1980) and was first modeled by Kopp and Pneumann (1976). Ongoing reconnection below the filament created progressively larger loops with hot plasma. In this flare, this was observed as an apparent southerly motion of the X-ray source located at the tops of the loops.

a) *Origin of Hard X-ray Footpoints and Hα Kernels*

In this section, we concentrate on the two hard X-ray bright points observed during peak 1 at $20^h55^m55^s$ (the story for peak 2 is qualitatively the same). The length of the loop connecting pixels *a* and *b* is estimated at 45,000 km. We recall that the light curves of pixel *a* and *b* are cotemporal to within 3 s. Requiring an Alfvén wave travel time from *a* to *b* along the loop of less than 3 s, we find $n_{10} \leq 0.02 B_2{}^2$, where density and magnetic field in the loop are expressed in units of 10^{10} cm^{-3} and 10^2 G. It appears difficult to satisfy the inequality with a plausible combination of n_{10} and B_2.[6] Thus we may ignore the theoretical possibility that there are two separate primary energy release sites, one at *a* and one at *b*: As no MHD connection could have caused their cotemporality, the latter would be *accidental*, and the probability of such a coincidence is small. The X-ray emission at *a* and *b* must rather be due to one single primary energy release site located somewhere in the loop. A thermal X-ray source as proposed by Brown, Melrose, and Spicer (1979) and Smith and Lilliequist (1979) can be ruled out: The travel time of a thermal conduction front from the top to a footpoint will be about 10 s or larger (Brown *et al.*). With its time resolution of 1.5 s, HXIS should have observed a bright (expanding) source between *a* and *b*, but none was seen.

These results imply that the two hard X-ray bright points were caused by thick target bremsstrahlung from fast electrons accelerated somewhere in the loop. These electrons may also generate Hα kernels as first elaborated by Brown (1973). Applying standard bremsstrahlung calculations, we derive a beam strength of electrons above 16 keV of $F_{16} \sim 3\times10^{35}$ s^{-1} and a corresponding power of $P_{16} \sim 10^{28}$ ergs s^{-1}. These (preliminary) figures are totals of both beams. The beams persisted for $\sim$30 s. Assuming that the acceleration region is not in a footpoint, the ratio of its brightness (I_{ac}) to that of a footpoint (I_{fp}) was observed to satisfy $I_{ac}/\ I_{fp} < 0.3$ at $\sim$20 keV. A thermal source with a continuously regenerated and escaping electron tail as proposed by Vlahos and Papadopoulos (1979) and Emslie (1981) is possible in principle, but its efficiency is found to be no larger than that of a thick target beam model (Brown 1971). Moreover, continuous regeneration of the tail at the required speed by Coulomb interactions is very difficult. It appears therefore that in this flare genuine acceleration occurred during peaks 1 and 2 down to about 16 keV. The nature of the acceleration mechanism and the consequences of the stability requirement on the reverse current will be analyzed later. The former is now restricted by the observed upper limit on I_{ac}/I_{fp}. It is difficult to accept Smith's (1980) conclusion that only a fraction 10^{-3} of the flare energy can be deposited into accelerated electrons, as it would imply that at least a total of 5×10^{32} ergs was already dissipated during the 60s comprising peaks 1 and 2.

b) *Temperature Structure and Energy Balance in the Thermal Phase*

Most of the radiation observed from about 21^h00^m onward can be explained by a hot, multitemperature plasma which is continuously heated. Table 1 gives an example of a (provisional) two-temperature fit to the spectrum observed by HXIS (integrated over the flare area). A temperature of 7×10^7 K is larger than ever found before during the thermal phase, and spectra from individual pixels indicate that possibly higher temperatures occurred. This two-temperature model fits the HXIS spectrum rather well, and it also accounts for the flux observed by HXRBS in the 26–52 keV channel. It predicts a Fe XXVI line flux consistent with what is observed by the Bent Crystal Spectrometer aboard *SMM* (R. Mewe and E. Antonucci 1980, private communication). We locate the hot plasma region at the top of those loops which are just being heated in the reconnection process; the cool component refers to lower-lying loops which had previously been heated, but have since cooled somewhat. This interpretation is supported by the $\sim$3″ displacement between the 3.5–8 keV and 16–30 keV emission (§ II*b*): A natural explanation is that the 16–30 keV emission emerges from a region $\sim$6000 km higher in the atmosphere than the 3.5–8 keV emission.

TABLE 1

TWO-TEMPERATURE ANALYSIS AT 21^h00^m

Region	T_e(K)	Y (cm^{-3})
Cool	2×10^7	5×10^{49}
Hot	7×10^7	1.3×10^{47}

[6]Since from our data the temperature at that time was about 2×10^7 K, the inequality implies a plasma β as small as $\sim 10^{-3}$ or less.

For a preliminary analysis of the energy balance, we shall assume that the hot region is homogeneous. From the observed 16–30 keV source size, we infer a volume for the hot component of $\sim 10^{27}$ cm^3 (within a factor 4); its density is then $n \sim 10^{10}$ cm^{-3}. The energy loss of the hot component is dominated by conduction; radiative losses are completely negligible. Using a length scale $L \sim 10^9$ cm (cf. Fig. 4), the classical conductive heat flux density turns out to be much larger than the *saturated* heat flux density, $nmv_t^3/4$. Assuming a saturated heat flux, the total energy loss rate from the hot component is $\sim 2 \times 10^{29}$ ergs s^{-1}, which implies a cooling time of ~ 2 s. As the observed decay time is much larger, it follows that this power was liberated in the hot source, presumably by ongoing reconnection. Note that the X-rays above 50 keV observed by HXRBS at 21^h00^m and later indicate that yet some electron acceleration took place besides heating. Likewise, the diffuse 16–30 keV X-ray patch observed during peaks 1 and 2 indicates that some heating was already going on then.

A similar two-temperature analysis (including the 26–52 keV channel of HXRBS) yields $T_{\rm cool} \sim 1.6 \times 10^7$ K and $T_{\rm hot} \sim 4 \times 10^7$ K at 21^h16^m. The hot component was still dominated by saturated conductive losses, and the dissipation rate at that time was $\sim 4 \times 10^{28}$ ergs s^{-1}. Whether the dissipation rates quoted equal the actual net dissipation rate going on in the flare will be analyzed in a later study. Factors to consider are (1) wave excitation, which may reduce the heat flux to a value below saturation, and (2) energy release in the cool component.

Finally, we note that an indication for the occurrence of very high temperatures and electron beams was found earlier in the flare of 1980 April 10, 09^h18^m (Hoyng *et al.* 1981).

It is a pleasure to thank Dr. J. Harvey for putting the KPNO magnetograms at our disposition and Dr. J. C. Brown for a critical reading of the manuscript. We are grateful to the US Air Weather Service Solar Observing Optical Network (SOON) and to Mr. J. Hirman at Boulder for making Hα filtergrams available to us.

REFERENCES

Brown, J. C. 1971, *Solar Phys.*, **18**, 489.
______. 1973, *Solar Phys.*, **31**, 143.
Brown, J. C., Melrose, D. B., and Spicer, D. S. 1979, *Ap. J.*, **228**, 592.
Emslie, A. G. 1981, *Ap. J.*, **245**, 711.
Heyvaerts, J., Priest, E. R., and Rust, D. M. 1976, *Ap. J.*, **216**, 123.
Hoyng, P., *et al.* 1981, *Ap. J.* (*Letters*), **244**, L153.
Kopp, R. A., and Pneuman, G. W. 1976, *Solar Phys.*, **50**, 85.
Kuperus, M., and Van Tend, W. 1981, *Solar Phys.*, in press.
Moore, R., McKenzie, D. L., Svestka, Z., and Widing, K. G. 1980, in *Solar Flares, A Monograph from Skylab Solar Workshop II*, ed. P. A. Sturrock (Boulder: Colorado Associated Universities), p. 341.
Orwig, L. E., Frost, K. J., and Dennis, B. R. 1980, *Solar Phys.*, **65**, 25.
Smith, D. F. 1980, *Solar Phys.*, **66**, 135.
Smith, D. F., and Lilliequist, C. G. 1979, *Ap. J.*, **232**, 582.
Spicer, D. S. 1977, *Solar Phys.*, **53**, 305.
van Beek, H. F., Hoyng, P., Lafleur, B., and Simnett, G. M. 1980, *Solar Phys.*, **65**, 39.
van Beek, H. F., *et al.* 1981, *Ap. J.* (*Letters*), **244**, L157.
Vlahos, L., and Papadopoulos, K. 1979, *Ap. J.*, **233**, 717.
Woodgate, B. E., *et al.* 1981, *Ap. J.* (*Letters*), **244**, L133.

A. Boelee, C. de Jager, A. Duijveman, P. Hoyng, H. Lafleur, Z. Svestka, and H. F. van Beek: Space Research Laboratory, Beneluxlaan 21, 3527 HS, Utrecht, The Netherlands

K. J. Frost and B. E. Woodgate: Laboratory for Astronomy and Solar Physics, NASA Goddard Space Flight Center, Greenbelt, MD 20771

M. E. Machado: Observatorio de Fisica Cosmica–CNIE, Av. Mitre 3100, 1663 San Miguel (Bs. As.), Argentina

D. M. Rust: American Science & Engineering, Inc., 955 Massachusetts Avenue, Cambridge, MA 02139

G. M. Simnett: Department of Space Research, P.O. Box 363, Birmingham B15 2TT, England